

Synthesis of Novel Fluorene-Based Poly(iminoarylene)s and Their Application to Buffer Layer in Organic Light-Emitting Diodes

Byung-Jun Jung,[†] Jeong-Ik Lee,[‡] Hye Yong Chu,[‡] Lee-Mi Do,[‡] and Hong-Ku Shim^{*,†}

Center for Advanced Functional Polymers, Department of Chemistry and School of Molecular Science (BK21), Korea Advanced Institute of Science and Technology, Tae-jon 305-701, Korea, and Basic Lab., Electronics and Telecommunications Research Institute (ETRI), Taejon 305-350, Korea

Received September 18, 2001; Revised Manuscript Received December 28, 2001

ABSTRACT: The fluorene-based poly(iminoarylene)s with triarylamine unit were simply synthesized from palladium-catalyzed polycondensation of 2,7-dibromo-9,9-di-*n*-alkylfluorene with primary amines such as aniline and *p*-toluidine. The polymers with high molecular weight were obtained and were thermally stable. The HOMO levels of the polymers (~ -5.1 eV) were close to the work function of ITO. Organic light-emitting diodes (OLEDs) of the form ITO/polymer/TPD/Alq₃/LiF/Al showed lower turn-on voltage ($V_T = 2.2$ V), the enhanced efficiency, and the higher maximum luminance at the higher current density (PFA1: 12 370 cd/m² at 427 mA/cm²) than those of the device without polymer ($V_T = 3.6$ V, 5790 cd/m² at 233 mA/cm²). It is expected that these polymers can be used as a buffer layer in OLEDs.

Introduction

For the past decade, organic light-emitting diodes (OLEDs) have attracted much attention from academia and industry because of their applications in large area flat-panel displays.^{1,2} Generally, OLEDs are thin-film multiplayer structures composed of a hole-transporting, an emitting, and an electron-transporting material sandwiched between two electrodes, which result in a good charge balance of electrons and holes. The most well-known hole-transporting material is *N,N*-diphenyl-*N,N*-bis(3-methylphenyl)-1,1'-biphenyl-4,4'-diamine (TPD), which is a triarylamine derivative.³ However, it has a low T_g (glass transition temperature) value (60 °C)⁴ and that causes crystallization and thermal breakdown during the operation of OLEDs.⁵ For that reason, the development of hole-transporting materials with high T_g is an important issue in OLED material synthesis. For example, starburst compounds⁶ and spiro compounds⁷ with high T_g were reported, and *N,N*-diphenyl-*N,N*-bis(α -naphthyl)benzidine (NPB) has been widely used instead of TPD.⁸ The high- T_g polymers containing a TPD unit were synthesized as well.⁹

To prevent the thermally morphological changes within the TPD layer, there have been approaches to enhance the interfacial stability between the anode and the hole-transporting layer by forming covalent chemical bonds to the indium–tin oxide (ITO) surface.¹⁰ A buffer layer such as copper phthalocyanine (CuPc) affects the stability of the interface.¹¹ Moreover, the buffer layer was inserted between ITO and hole-transporting layer (HTL) to lower the operating voltage, because its highest occupied molecular orbital (HOMO) energy level is close to the work function of ITO. Other buffer layers such as the hole-transporting polymer layer mixed with a strong acceptor or starburst amine layer doped with a strong acceptor were reported.¹²

The triarylamine-based hole-transporting materials were usually synthesized by Ullmann coupling⁸ or Pd-

catalyzed amination.^{9b,13} However, the polymerization using these reactions is difficult. Alternatively, several polymers containing an arylamine group were synthesized by Suzuki coupling,¹⁴ Wittig–Horner reaction,¹⁵ and condensation⁹ with already synthesized arylamine monomer. Among them, fluorene-based copolymers prepared by using the Suzuki coupling reaction showed high hole mobility^{14a} as well as good thermal stability with high T_g .^{14b} Especially, they have great potential to be applied as a hole-transporting layer or a hole injection layer (buffer layer) in OLED because they have a close work function to ITO.^{14c}

Through the development of the synthetic method of triarylamine (reaction yield > 99%),^{16a} Kanbara et al. succeeded in the Pd-catalyzed polycondensation using the special reaction ligand.^{16b} This reaction easily gives a triarylamine unit in the polymer main chain, and therefore, it can provide facile and alternative route to prepare new fluorene-based copolymers with arylamine. In this paper, we present new fluorene-based poly(iminoarylene)s with a triarylamine unit synthesized by using Pd-catalyzed polycondensation and their characteristics related to their structures. Moreover, we have applied the synthesized polymers as a buffer layer in OLED and achieved improved device performance. The detailed explanation for improved device performance is also discussed.

Experimental Section

Measurements. NMR spectra were recorded on a Bruker AVANCE 400 spectrometer with tetramethylsilane as internal reference. The number- and weight-average molecular weight of polymers were determined by gel permeation chromatography (GPC) on a Waters GPC-150C instrument, using THF as eluent and polystyrene as standard. TGA and DSC of polymers were performed under a nitrogen atmosphere at a heating rate of 10 °C/min with a Dupont 9900 analyzer. UV–vis spectra were measured by using a Jasco V-530 UV/vis. Spectrometer and photoluminescence spectra by using a Spex Fluorolog-3 spectrofluorometer with spin-coated films at room temperature. Cyclic voltammetry was performed on an AUTOLAB/PGSTAT12 with a three-electrode cell in a solution of Bu₄NBF₄ (0.10 M) in acetonitrile at a scan rate of 50 mV/s.

[†] Korea Advanced Institute of Science and Technology.

[‡] Electronics and Telecommunications Research Institute.

* To whom correspondence should be addressed. Tel +82-42-869-2827; Fax +82-42-869-2810; e-mail hkshim@mail.kaist.ac.kr.

Ionization potentials (IP) of polymers were obtained using atmospheric photoelectron spectroscopy (RIKEN Keiki AC-2). Electroluminescence spectra were obtained with a Minolta CS-1000. The current/voltage and luminescence/voltage characteristics were taken with a current/voltage source (Keithley 238) and a Minolta LS-100.

Materials. Aniline, *p*-toluidine, α -naphthylamine, 2,7-dibromofluorene, toluene (99.8%, anhydrous), sodium *tert*-butoxide (NaO-*t*-Bu), tris(dibenzylideneacetone)dipalladium(0) (Pd₂(dba)₃), and tri-*tert*-butylphosphine (P(*t*-Bu)₃) were purchased from Aldrich. All chemicals were used without further purification. The monomers 2,7-dibromo-9,9-di-*n*-hexylfluorene and 2,7-dibromo-9,9-di-*n*-octylfluorene were prepared by reacting 2,7-dibromofluorene with 1-bromohexane and 1-bromooctane according to a literature procedure.¹⁷

Polymerization. a. PFA 1. A mixture of 2,7-dibromo-9,9-di-*n*-hexylfluorene (1.27 g, 2.58 mmol) and aniline (0.256 g, 2.58 mmol) was dissolved in toluene (25 mL). NaO-*t*-Bu (0.744 g, 7.74 mmol), Pd₂(dba)₃ (0.060 g, 0.065 mmol), and P(*t*-Bu)₃ (0.079 g, 0.39 mmol) were added to the solution at room temperature. The reaction mixture was stirred at 100 °C for 36 h under N₂. After cooling to room temperature, the mixture was quenched by adding aqueous ammonia (50 mL) and the product was extracted with CHCl₃. The organic fraction was concentrated and reprecipitated from CHCl₃/methanol several times. After filtration and being vacuum-dried, dark yellow PFA1 (0.94 g 86% yield) was obtained. Anal. Found: C, 87.71; H, 9.00; N, 3.29. Calcd for (C₃₁H₃₇N)_n: C, 87.89; H, 8.80; N, 3.31. ¹H NMR (400 MHz in CDCl₃, ppm): 7.58 (d, 2H), 7.21 (d, 2H), 7.12 (s, 4H), 6.68 (m, 3H), 1.75 (br, 4H), 1.26–0.59 (m, 22H). ¹³C NMR (100 MHz in CDCl₃, ppm): 151.8, 148.3, 146.4, 136.0, 129.0, 123.3, 123.0, 121.9, 119.6, 118.9, 55.0, 40.2, 31.6, 29.6, 23.9, 22.5, 14.1.

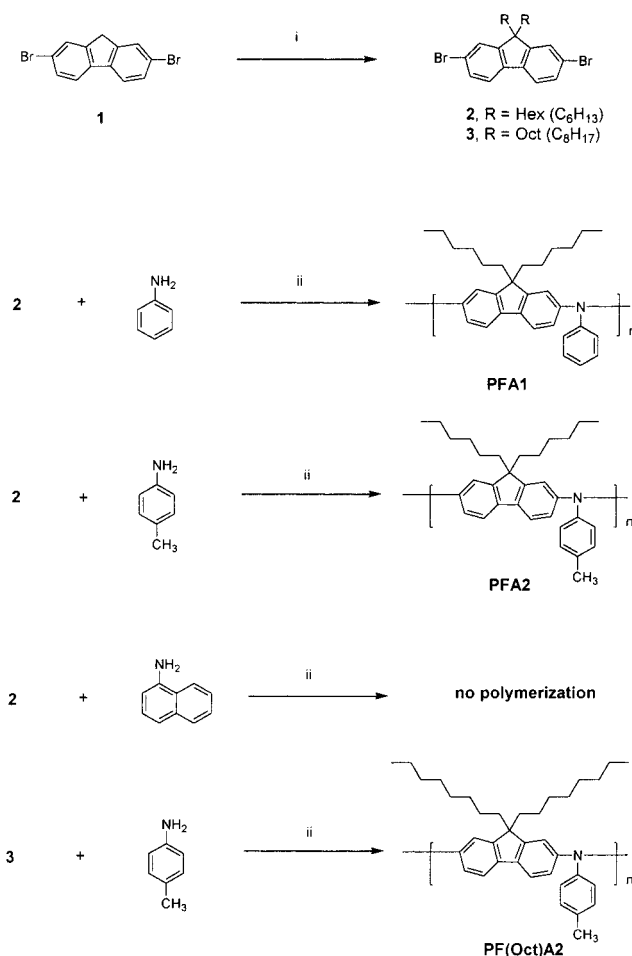
b. PFA2. A mixture of 2,7-dibromo-9,9-di-*n*-hexylfluorene (1.29 g, 2.62 mmol) and *p*-toluidine (0.281 g, 2.62 mmol) was dissolved in toluene (25 mL). NaO-*t*-Bu (0.755 g, 7.86 mmol), Pd₂(dba)₃ (0.060 g, 0.065 mmol), and P(*t*-Bu)₃ (0.079 g, 0.39 mmol) were added to the solution at room temperature. The reaction and workup procedure were carried out as described for PFA1. The greenish gray PFA2 (0.80 g, 70% yield) was obtained. Anal. Found: C, 87.66; H, 9.24; N, 3.10. Calcd for (C₃₂H₃₉N)_n: C, 87.82; H, 8.98; N, 3.20. ¹H NMR (400 MHz in CDCl₃, ppm): 7.43 (d, 2H), 7.10 (s, 2H), 7.05 (s, 4H), 6.67 (d, 2H), 2.32 (s, 3H), 1.75 (br, 4H), 1.26–0.59 (m, 22H). ¹³C NMR (100 MHz in CDCl₃, ppm): 151.7, 146.5, 145.8, 135.7, 131.8, 129.7, 123.8, 122.7, 119.4, 118.3, 54.9, 40.2, 31.7, 29.7, 23.9, 22.5, 20.8, 14.1.

c. PF(Oct)A2. A mixture of 2,7-dibromo-9,9-di-*n*-octylfluorene (1.10 g, 2.03 mmol) and *p*-toluidine (0.218 g, 2.03 mmol) was dissolved in toluene (25 mL). NaO-*t*-Bu (0.585 g, 6.09 mmol), Pd₂(dba)₃ (0.047 g, 0.051 mmol), and P(*t*-Bu)₃ (0.062 g, 0.30 mmol) were added to the solution at room temperature. The reaction and workup procedure were carried out as described for PFA1. The greenish gray PF(Oct)A2 (0.72 g, 72% yield) was obtained. Anal. Found: C, 87.27; H, 9.84; N, 2.90. Calcd for (C₃₆H₄₇N)_n: C, 87.57; H, 9.59; N, 2.84. ¹H NMR (400 MHz in CDCl₃, ppm): 7.50 (d, 2H), 7.10 (s, 2H), 7.03 (s, 4H), 6.66 (d, 2H), 2.32 (s, 3H), 1.76 (br, 4H), 1.26–0.59 (m, 30H). ¹³C NMR (100 MHz in CDCl₃, ppm): 151.7, 146.6, 145.8, 135.7, 131.8, 129.7, 123.8, 122.7, 119.5, 118.4, 55.0, 40.2, 31.9, 30.1, 29.5, 29.3, 24.0, 22.7, 20.8, 14.1.

Results and Discussion

Synthesis and Characterization of Polymers. The simple synthesis of polymers shown in Scheme 1 proceeded via a Pd-catalyzed polycondensation of 2,7-dibromo-9,9-di-*n*-hexyl(or octyl)fluorene with primary amines such as aniline, *p*-toluidine, and α -naphthylamine. The used ligand was P(*t*-Bu)₃, which was reported as an effective ligand in polycondensation.¹⁶ The polymerization with aniline and *p*-toluidine was successful, but the polymerization with α -naphthylamine failed because of the steric hindrance. The polymers

Scheme 1. Synthetic Route for Fluorene-Based Poly(iminoarylene)s^a



^a Reagents and conditions: (i) 1-bromohexane (2) (or 1-bromooctane(3)), toluene, H₂O, NaOH, tetra(*n*-butyl)ammonium bromide, 60 °C; (ii) toluene, NaO-*t*-Bu, Pd₂(dba)₃, P(*t*-Bu)₃, 100 °C.

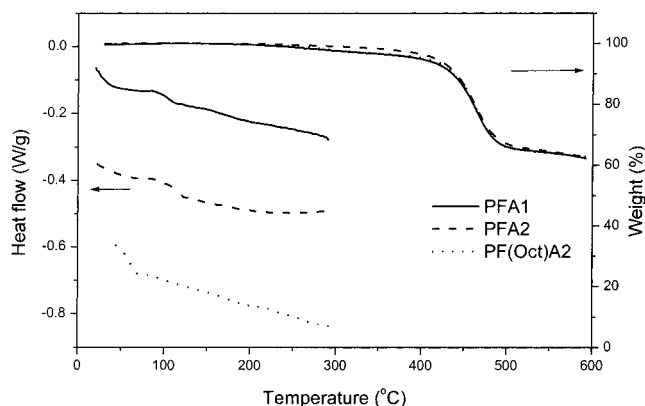


Figure 1. TGA and DSC curves of PFA1, PFA2, and PF(Oct)A2.

(PFA1, PFA2, PF(Oct)A2) were obtained in good yields (over 70%) and were well characterized by ¹H NMR, ¹³C NMR, and elemental analyses. The weight-average molecular weights (*M*_w) of PFA1, PFA2, and PF(Oct)A2, determined by gel permeation chromatography (GPC) based on polystyrene standards using THF as an eluent, were 35 800, 37 700, and 29 100 with polydispersity index of 2.56, 3.02, and 2.37, respectively, which were comparable to those (*M*_w = 10 000–30 000) of the fluorene-based alternating copolymers synthesized via

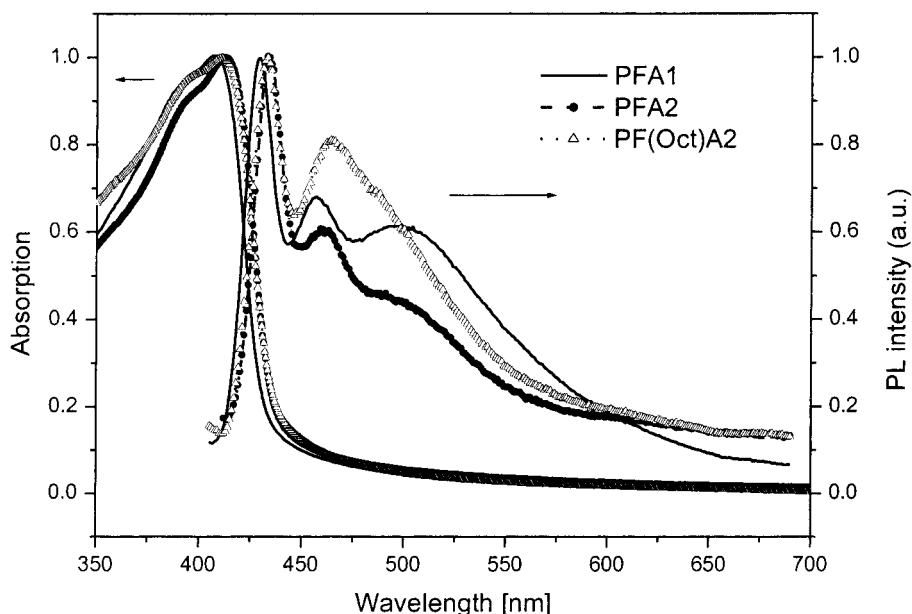


Figure 2. UV-vis absorption and photoluminescence spectra of PFA1, PFA2, and PF(Oct)A2.

Table 1. Physical Properties of the Polymers

polymer	yield (%)	M_n	M_w	PDI	T_g (°C)	T_d^{5a} (°C)
PFA1	86	14 000	35 800	2.56	107	394
PFA2	70	12 500	37 700	3.02	120	413
PF(Oct)A2	72	12 300	29 100	2.37	65	401

^a Temperature resulting in 5% weight loss based on initial weight.

Suzuki coupling.^{14a} All polymers were very soluble in common organic solvents such as chloroform, THF, and 1,2-dichloroethane and showed good film-forming quality. The alkyl chain substitutions at a remote C₉ site of fluorene improved the solubility of the polymers.¹⁸ Moreover, the substitution provides high molecular weight and processability to the polymers.

The thermal properties of the polymers were determined by thermal gravimetric analysis (TGA) and differential scanning calorimetry (DSC). All polymers showed good thermal stability (see Figure 1) as weight loss was less than 5% on heating to about 400 °C under a nitrogen atmosphere. PFA1 and PFA2 with a hexyl group showed the glass transition temperatures (T_g) at 107 and 120 °C, respectively, but PF(Oct)A2 with the octyl group at 65 °C. PF(Oct)A2 with longer alkyl chains showed a lower T_g because of the expansion of free volume. The T_g difference between PFA1 and PFA2 was caused by the steric hindrance of the methyl group. Compared with the previous reported fluorene-based alternating copolymers with an octyl group,^{14b} PF(Oct)A2 shows a lower T_g . However, a shorter alkyl chain, the hexyl group, gives these fluorene-based poly(iminoarylene)s not only good solubility that enable to obtain high molecular weight but also good thermal stability comparable to those reported. The polymer properties are summarized in Table 1.

Figure 2 shows the UV-vis absorption spectra and the photoluminescence (PL) spectra of the polymers in thin films on quartz plates. The maximum absorption of PFA1 appeared at 406 nm and the absorption edge of PFA1 at 430 nm. For PFA2 and PF(Oct)A2, the maximum absorptions appeared at 411 nm and the absorption edges at 435 nm. With an excitation wavelength of 390 nm, the PL spectra of PFA1, PFA2, and

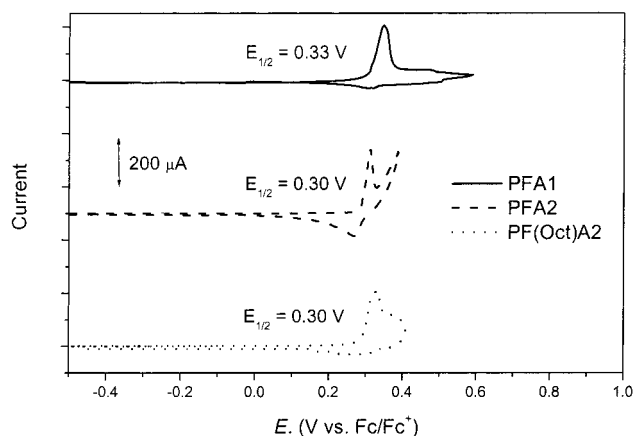


Figure 3. Cyclic voltammogram (oxidation) of polymers (0.10 M Bu₄NBF₄ in CH₃CN, scan 50 mV/s).

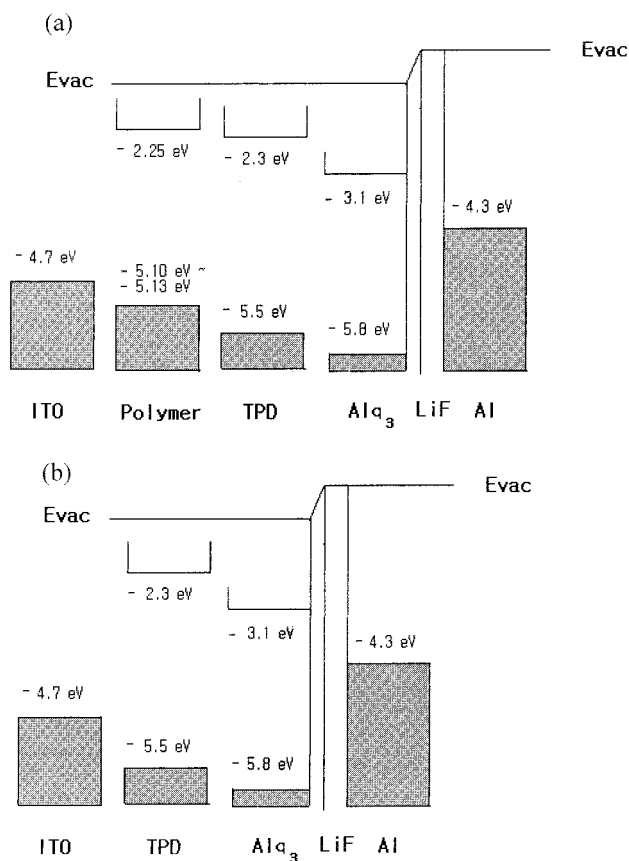
PF(Oct)A2 showed the maximum peaks at 429, 433, and 433 nm, respectively. The PL maximum peaks are well matched to the absorption edges. UV and PL spectra of PFA2 are nearly identical to those of PF(Oct)A2 and are slightly red-shifted respect to those of PFA1. Owing to the attachment the methyl group, which is an electron-donating group, to the phenyl ring, the electronic state of the polymers is changed. However, the alkyl chain substitutions at the remote C₉ site of fluorene seldom gave any changes in the electronic states of these polymers.

Figure 3 shows the cyclic voltammograms (CV) of the polymers, which were obtained from the films prepared by dip-coating the polymer solutions onto Pt wire. The polymers showed reversible peak under oxidation process, which indicates their electrochemical stability in the hole-carrying process. The oxidation potentials of PFA2 and PF(Oct)A2 ($E_{1/2} = 0.30$ V vs Fc/Fc⁺) were slightly lower than that of PFA1 ($E_{1/2} = 0.33$ V vs Fc/Fc⁺), which may be rationalized by the electron-donating ability of arenes to the nitrogen.^{4,6d,9b} The energy levels of the polymers were calculated using the ferrocene (FOC) value of -4.8 eV as standard.¹⁹ The HOMO levels, which were calculated from CV, are similar to the ionization potentials (IP) which was measured by a

Table 2. Optical and Electrochemical Properties of the Polymers

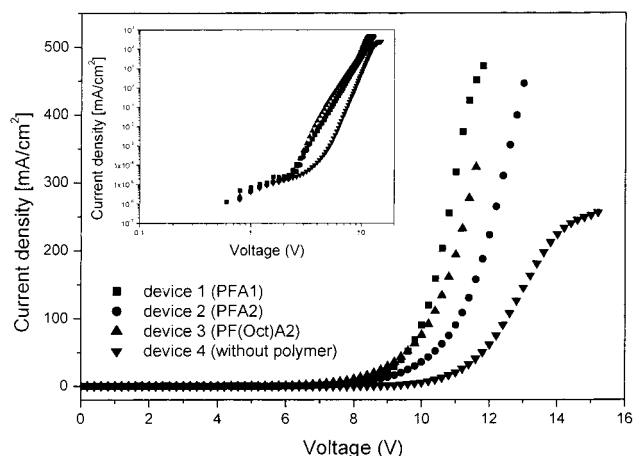
polymer	λ_{abs} (nm) ^a	λ_{PL} (nm) ^a	band gap ^b (eV)	$E_{1/2}$ (V vs Fc/Fc ⁺)	HOMO (eV) ^c	LUMO (eV) ^d	IP (eV) ^e
PFA1	406	429	2.88	0.33	-5.13	-2.25	-5.18
PFA2	411	433	2.85	0.30	-5.10	-2.25	-5.08
PF(Oct)A2	411	433	2.85	0.30	-5.10	-2.25	-5.07

^a Wavelength of maximum of absorption and emission (spin-coated film). ^b Calculated from the absorption edge of the UV-vis spectrum. ^c HOMO energy level was calculated by using ferrocene value of 4.8 eV below the vacuum level. ^d Estimated from the HOMO and band gap. ^e Measured by a RIKEN Keiki AC-2.

**Figure 4.** Schematic view of the device structures: (a) ITO/polymer/TPD/Alq₃/LiF/Al (device 1, PFA1; device 2, PFA2; and device 3, PF(Oct)A2); (b) ITO/TPD/Alq₃/LiF/Al (device 4).

RIKEN Keiki AC-2. The optical and electrochemical properties of the polymers are listed in Table 2. The polymers showed HOMO levels of ~ -5.1 eV, which are higher than those of TPD (~ -5.5 eV) or NPB (~ -5.7 eV) which are small organic hole-transporting materials.^{4a} Such energy levels may provide a closer match to the work function of ITO when they are used as hole-injection materials in OLEDs.

Performance of OLED Devices Using Polymers as the Buffer Layer. OLEDs (devices 1–3) of the configuration ITO/polymer (~ 10 nm)/TPD(50 nm)/Alq₃(60 nm)/LiF(1 nm)/Al(100 nm) were fabricated, where Alq₃, tris(8-quinolinolato)aluminum, was inserted as an emitting material and electron-transfer material. For comparison, a typical device (device 4) without the polymer was fabricated at the same time (Figure 4). The polymer layers were prepared by spin-coating the polymer solutions (2 mg/mL) on ITO at 2000 rpm and other material layers by evaporation. The devices showed Alq₃ emission of 525 nm. Figure 5 shows the

**Figure 5.** Voltage-current density characteristics of the devices. Inset: logarithmic voltage-current density characteristics of the devices.**Table 3. Performance Characteristics of the Devices**

device	turn-on voltage (V)	photometric efficiency [cd/A] at 20 mA/cm ²	operating voltage (V) at 300 cd/m ²	max brightness [cd/m ²]	current density at max brightness [mA/cm ²]
1	2.2	3.70	8.3	12 370	472
2	2.2	3.89	8.4	11 930	446
3	2.2	3.98	7.8	10 800	323
4	3.6	3.56	10.3	5 790	233

voltage-current density characteristics of the devices, and Figure 6 shows the current density-luminance characteristics of the devices. Table 3 summarizes the device data. Clearly, the thin polymer buffer layer significantly reduces the turn-on voltage (V_T) from 3.6 to 2.2 V as CuPc does,^{4a,11} and devices 1–3 with the polymers showed a much lower operating voltage (at 300 cd/m²) than device 4 without polymer. These behaviors may be due to the low-energy barrier. The difference of the operating voltage in devices 1–3 was caused by the slight difference of the polymer layer thickness. In addition, enhanced efficiencies were observed due to the presence of polymers and the photometric efficiencies slowly decreased in device 1–3 against to device 4 as increasing the current density (see Figure 6). The efficiency was not improved, when CuPc was used as the buffer layer.^{4a,11} The efficiency is a more complicated problem, and not only energy level but also the interfaces between each layer must be considered. We guess that the thin polymer layers enable to easily transport carrier and improve the adhesion between ITO and organic layer. The maximum luminance of the devices 1, 2, 3, and 4 were obtained as 12 370, 11 930, 10 800, and 5790 cd/m², respectively. Because each device 1 and 2 consists of PFA1 and PFA2 with high T_g (109 and 120 °C, respectively), the devices showed the higher maximum luminance with higher efficiency and stable operation at high current density. The thermally stable fluorene-based poly(iminoarylene)s can supply the lack of thermal stability of TPD with which the device showed slightly higher efficiency^{4a} than the device with NPB. This hole-transporting system (fluorene-based poly(iminoarylene)s/TPD) will be useful for red OLEDs, which suffer from low efficiencies and high operating voltages.²⁰

HTL Morphology. To investigate the effect of polymer buffer layer on HTL interface morphology, TPD

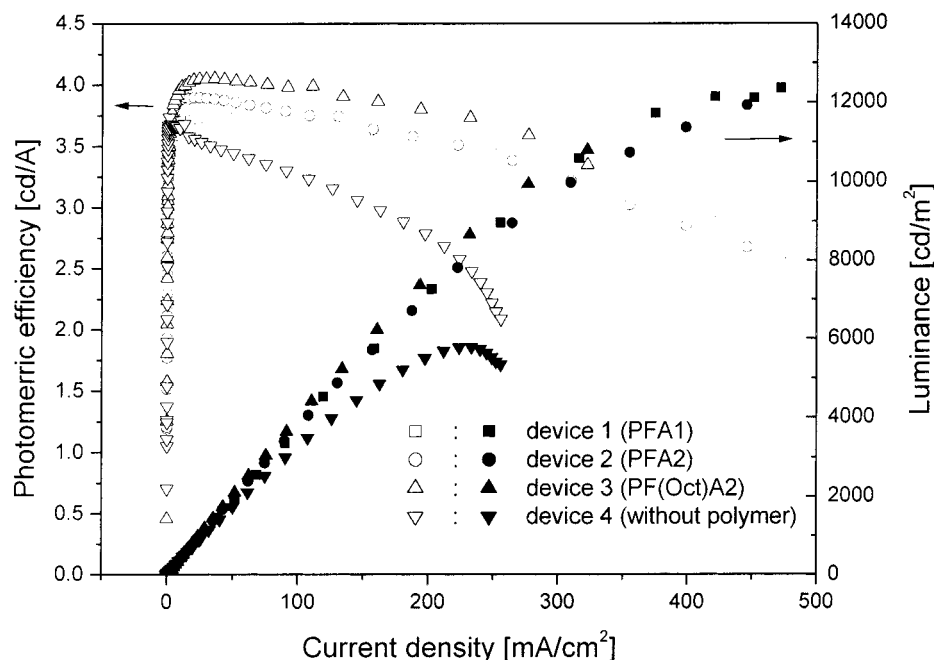


Figure 6. Current density–luminance and current density–photometric efficiency plots of the devices.

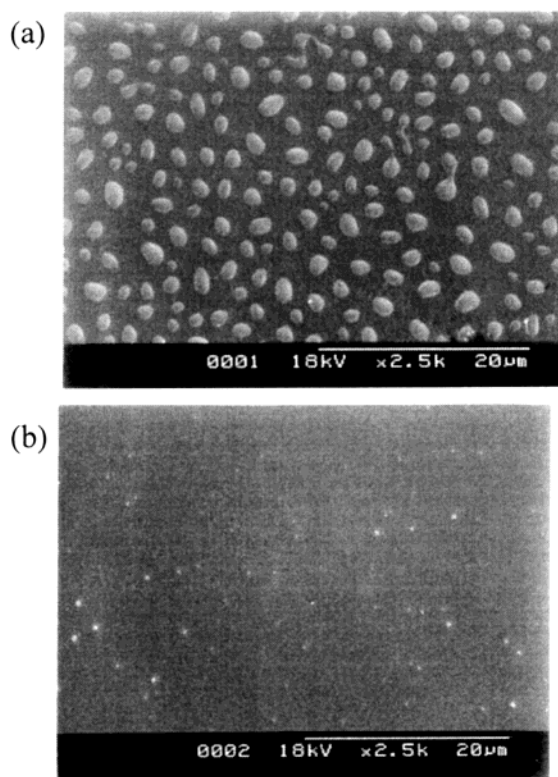


Figure 7. Scanning electron microscope photographs of TPD films: (a) TPD film evaporated on bare ITO, followed by heating at 80 °C for 1 h; (b) TPD film evaporated on ITO coated with PFA1, followed by heating at 80 °C for 1 h.

films were vacuum-deposited on a bare ITO or PFA1-coated ITO. The samples were heated at 80 °C under N₂ for 1 h. The film surface morphology was imaged by SEM (Figure 7). The TPD hemispherical islands formed on a bare ITO, but the amorphous and homogeneous TPD film state was maintained on the PFA1-coated ITO. These results definitely effect the current density–luminance characteristics of the devices; we suppose that the PFA1 and PFA2 polymers with high *T_g* improve

the durability of HTL on Joule heat, which arises in OLED operations, and enable OLED to show better performance.

Conclusions

We synthesized the fluorene-based poly(iminoarylene)s with a triarylamine unit by the Pd-catalyzed polycondensation. The synthesized polymers were soluble in common organic solvents and showed high molecular weight and good film quality. The HOMO levels of the polymers (~−5.1 eV) matched well with the ITO anode. The OLEDs consisting of these polymers as a buffer layer showed the lower *V_T*, enhanced efficiency, and higher maximum luminance because polymer layers enhance the hole injection and improve the thermal stability of HTL.

Acknowledgment. This work was supported by the Center for Advanced Functional Polymers (CAFPoly) through KOSEF and the Ministry of Information and Communications, Republic of Korea. We thank K.-S. Kim and Prof. J.-B. Kim for the scanning electron microscopy images.

References and Notes

- (1) Tang, C. W.; Vanslyke, S. A. *Appl. Phys. Lett.* **1987**, *51*, 913.
- (2) Friend, R. H.; Gymer, R. W.; Holmes, A. B.; Burroughes, J. H.; Marks, R. N.; Taliani, C.; Bradley, D. D. C.; Santos, D. A. Dos; Bredas, J. L.; Logdlund, M.; Salaneck, W. R. *Nature (London)* **1999**, *397*, 121.
- (3) (a) Tang, C. W.; Vanslyke, S. A.; Chen, C. H. *J. Appl. Phys.* **1989**, *65*, 3610. (b) Adachi, C.; Tsutsui, T.; Saito, S. *Appl. Phys. Lett.* **1989**, *55*, 1489.
- (4) (a) O'Brien, D. F.; Burrow, P. E.; Forest, R. S.; Koene, B. E.; Loy, D. E.; Thompson, M. E. *Adv. Mater.* **1998**, *10*, 1108. (b) Koene, D. E.; Loy, D. E.; Thompson, M. E. *Chem. Mater.* **1998**, *10*, 2235.
- (5) Zhou, X.; He, J.; Liao, L. S.; Lu, M.; Ding, X. M.; Hou, X. Y.; Zhang, X. M.; He, X. Q.; Lee, S. T. *Adv. Mater.* **2000**, *12*, 265.
- (6) (a) Kuwabara, Y.; Ogawa, H.; Inada, H.; Noma, N.; Sirota, Y. *Adv. Mater.* **1994**, *6*, 677. (b) Thelakkat, M.; Schmidt, H. W. *Adv. Mater.* **1998**, *10*, 219. (c) Katsuma, K.; Shirota, Y. *Adv. Mater.* **1998**, *10*, 223. (d) Wu, I. Y.; Lin, J. T.; Tao, Y. T.; Balasubramaniam, E. *Adv. Mater.* **2000**, *12*, 668.

- (7) (a) Bach, U.; Cloedt, K. D.; Spreitzer, H.; Gratzel, M. *Adv. Mater.* **2000**, *12*, 1060. (b) Spreitzer, H.; Vestweber, H.; Stobel, P.; Becker, H. *Proc. SPIE* **2001**, *4105*, 12.
- (8) VanSlyke, S. A.; Chen, C. J.; Tang, C. W. *Appl. Phys. Lett.* **1996**, *69*, 2160.
- (9) (a) Son, J. M.; Mori, T.; Ogino, K.; Sato, H.; Ito, Y. *Macromolecules* **1999**, *32*, 4849. (b) Bellmann, E.; Shaheen, S. E.; Grubbs, R. H.; Marder, S. R.; Kippelen, B. N.; Peyghambarian, B. *Chem. Mater.* **1999**, *11*, 399. (c) Schmitz, C.; Posch, P.; Thelakkat, M.; Schmidt, H.-W.; Montali, A.; Feldman, K.; Smith, P.; Weder, C. *Adv. Funct. Mater.* **2001**, *11*, 41.
- (10) (a) Cloncalves-Conto, S.; Carrard, M.; Si-Ahmed, L.; Zuppiroli, L. *Adv. Mater.* **1999**, *11*, 112. (b) Cui, J.; Huang, Q.; Wang, Q.; Marks, T. J. *Langmuir* **2000**, *17*, 2051. (c) Bellmann, E.; Jabbour, G. E.; Grubbs, R. H.; Peyghambarian, N. *Chem. Mater.* **2000**, *12*, 1349.
- (11) (a) Shi, J.; Tang, C. W. *Appl. Phys. Lett.* **1997**, *70*, 1665. (b) Shi, J.; Tang, C. W. U.S. Patent 5554450, 1996.
- (12) (a) Sato, Y.; Ogata, T.; Kido, J. *Proc. SPIE* **2001**, *4105*, 134. (b) Zhou, X.; Blochwitz, J.; Pfeiffer, M.; Nollau, A.; Fritz, T.; Leo, K. *Adv. Funct. Mater.* **2001**, *11*, 310.
- (13) Bellmann, E.; Shaheen, S. E.; Thayumanavan, S.; Barlow, S.; Grubbs, R. H.; Marder, S. R.; Kippelen, B.; Peyghambarian, N. *Chem. Mater.* **1998**, *10*, 1668.
- (14) (a) Redecker, M.; Bradley, D. D. C.; Inbasekaran, M.; Wu, W. W.; Woo, E. P. *Adv. Mater.* **1999**, *11*, 241. (b) Bernius, M. T.; Inbasekaran, M.; Woo, E. P.; Wu, W. W.; Wujkowski, L. *J. Mater. Sci., Mater. El.* **2000**, *11*, 116. (c) He, Y.; Kanicki, J. *Appl. Phys. Lett.* **2000**, *76*, 661. (d) Bernius, M. T.; Woo, E. P.; Wujkowski, L. L.; Inbasekaran, M. W. O. Patent 00 06665, 2000.
- (15) (a) Rost, H.; Horhold, H. H.; Kreuder, W.; Spreitzer, H. *Proc. SPIE* **1997**, *3148*, 373. (b) Kreuder, W.; Horhold, H. H.; Rost, H. U.S. Patent 5814244, 1998.
- (16) (a) Yamamoto, T.; Nishiyama, M.; Koie, Y. *Tetrahedron Lett.* **1998**, *39*, 2367. (b) Kanbara, T.; Oshima, M.; Imaysu, T.; Hasegawa, K. *Macromolecules* **1998**, *31*, 8725.
- (17) (a) Woo, E. P.; Inbasekaran, M.; Shiang, W.; Roof, G. R. WO 99 05184, 1997. (b) Lee, J. K.; Klaerner, G.; Miller, R. D. *Chem. Mater.* **1997**, *11*, 11083.
- (18) Klaerner, G.; Miller, R. D. *Macromolecules* **1998**, *31*, 2007.
- (19) Pommerehe, J.; Vestweber, H.; Guss, W.; Mahrt, R. F.; Bassler, H.; Porsch, M.; Daub, J. *Adv. Mater.* **1995**, *7*, 55.
- (20) (a) Chen, C. H.; Tang, C. W.; Shi, J. *Macromol. Symp.* **1997**, *125*, 1. (b) Kwaong, R. C.; Sibley, S.; Dubovoy, T.; Baldo, M.; Forrest, S. R.; Thompson, M. E. *Chem. Mater.* **1999**, *11*, 3709.

MA0116405